



Combination of tensor network states and Green's function Monte Carlo

Mingpu Qin 

*Key Laboratory of Artificial Structures and Quantum Control, School of Physics and Astronomy,
Shanghai Jiao Tong University, Shanghai 200240, China*

 (Received 21 June 2020; revised 9 September 2020; accepted 10 September 2020; published 24 September 2020)

We propose an approach to study the ground state of quantum many-body systems in which tensor network states, specifically projected entangled pair states (PEPSs), and Green's function Monte Carlo (GFMC) are combined. PEPSs, by design, encode the area law which governs the scaling of entanglement entropy in quantum systems with short-range interactions but are hindered by the high computational complexity scaling with bond dimension D . GFMC is a highly efficient method, but it usually suffers from the infamous negative sign problem which can be avoided by the fixed-node approximation in which a guiding wave function is utilized to modify the sampling process. The trade-off for the absence of the negative sign problem is the introduction of systematic error by the guiding wave function. In this work, we combine these two methods, PEPS and GFMC, to take advantage of both of them. PEPSs are very accurate variational wave functions, while at the same time, only contractions of the single-layer tensor network are necessary in GFMC, which reduces the cost substantially. Moreover, energy obtained in GFMC is guaranteed to be variational and lower than the variational energy of the guiding PEPS wave function. Benchmark results of the J_1 - J_2 Heisenberg model on the square lattice are provided.

DOI: [10.1103/PhysRevB.102.125143](https://doi.org/10.1103/PhysRevB.102.125143)

I. INTRODUCTION

One of the most challenging tasks in condensed-matter physics is to understand the many-body effect in strongly correlated quantum systems, in which numerous exotic phenomena emerge [1–4]. Because an exact solution for a strongly correlated system is rare [5], most studies of these systems rely on numerical tools nowadays. The density matrix renormalization group (DMRG) [6,7] is one of the most successful methods in the study of strongly correlated systems. DMRG is extremely accurate for one-dimensional (1D) quantum systems [8,9]. Shortly after the introduction of DMRG in 1992 [6], it was realized that the underlying wave functions are matrix product states (MPSs) [10], which can be viewed as a generalization of the seminal state introduced by Affleck, Kennedy, Lieb and Tasaki (AKLT) [11]. The concept of MPSs can be traced back at least to 1968 [12]. It was found that MPSs capture the entanglement structure of the ground state of 1D quantum systems and this results in the high accuracy of DMRG [13]. The adoption of concepts from the field of quantum information, entanglement, for example, has inspired the development of the tensor network states (TNSs) [14]. These advances provide us useful tools to both identify [15] and classify [16,17] quantum phases.

DMRG can also provide accurate results for systems on narrow cylinders with a large enough bond dimension [18–22] but has difficulty for a real two-dimensional (2D) system [23]. A natural generalization of MPSs to 2D, projected entangled pair states (PEPSs) [24], can overcome the difficulty [25–29]. It can be proved that the entanglement entropy in PEPS satisfies the area law [24] which is required to faithfully

represent the ground state of 2D quantum systems [13] (when a Fermi surface is present [30], there is a logarithm correction to area law for the ground state, which PEPS fails to capture.). However, in contrast to D^3 scaling of complexity in MPSs, the computational cost is as high as D^{12} [26,31,32] in PEPSs. The heavy scaling of computational resources with bond dimension in PEPSs hampers the reach to large bond dimension, which is essential to resolve possible competing states in the low-energy manifold of certain strongly correlated systems, e.g., the antiferromagnetic Heisenberg model on Kagome lattice [19,29,33–36].

Quantum Monte Carlo (QMC) [31,37–39] is a widely used methodology in the study of strongly correlated many-body systems. In general, the computational complexity in QMC scales algebraically with system size, which makes it an efficient approach. However, with few exceptions [31], the direct application of the Monte Carlo method in many-body systems suffers from the infamous negative sign problem [40,41]. One strategy to overcome the negative sign problem is to take advantage of the trade-off between variance and bias, which is the principle behind fixed-node approximation in Green's function Monte Carlo (GFMC) [42,43] (also called diffusion Monte Carlo [44] in the literature) and the constrained path approximation in auxiliary field quantum Monte Carlo [45]. The price to pay is the introduction of systematic error or bias in the result. Empirically, different forms of guiding [35,46–48] or trial wave functions [49,50] can be chosen to give high accuracy for certain systems.

In this work, we combine PEPS and GFMC to take advantage of both of them. We take PEPS as the guiding wave function in the GFMC calculation. As we will discuss later,

in our method, only contraction of the single-layer tensor network is required, which highly reduces the computational complexity in the PEPS part. At the same time, PEPSs are very accurate variational wave functions, with which the systematic error can be reduced in GFMC.

II. MODELS

For concreteness, we take the $S = 1/2$ J_1 - J_2 Heisenberg model on a square lattice as an example to describe the method. The Hamiltonian is as follows:

$$H = J_1 \sum_{\langle i,j \rangle} S_i S_j + J_2 \sum_{\langle\langle i,j \rangle\rangle} S_i S_j, \quad (1)$$

where S_i is the spin operator on site i . $\langle i, j \rangle$ and $\langle\langle i, j \rangle\rangle$ represent nearest- and next-nearest- neighbor interactions, respectively. We consider antiferromagnetic interactions for both J_1 and J_2 and set J_1 as the energy unit. For simplicity, we study the system on a square lattice with open boundary conditions (OBCs). The J_1 - J_2 Heisenberg model is widely investigated in the exploration of the frustration effect in quantum systems [51–53]. When J_2 is absent, the model can be solved with QMC without suffering from the negative sign problem [54–56]. The ground state is known to have long-range antiferromagnetic (AF) order, i.e., Néel order. In the other limit when $J_1 = 0$, the system decouples into two independent square lattices, and an infinitesimal J_1 can drive the ground state into the striped AF order. Between these two limits, the nature of the ground state is still under extensive debate [57–65] in the vicinity of $J_2/J_1 = 0.5$, where the system is maximally frustrated in the sense that in the classical limit, the J_1 - J_2 Ising model has a macroscopic degenerate ground state.

III. PROJECTED ENTANGLED PAIR STATES

To construct a PEPS, we put a rank 5 tensor $A_{ldru}^{[\sigma]}$ on each vertex of the square lattice [see Fig. 1(b)], where σ is the physical degree of freedom with dimension d , while l, d, r, u are the auxiliary degrees of freedom with dimension D [24]. Contracting the auxiliary degrees of freedom gives the PEPS wave function

$$\psi = \sum_{\{\sigma\}} \text{Tr}(A^{[\sigma_0]} A^{[\sigma_1]} \dots A^{[\sigma_{N-1}]}) |\sigma_0, \sigma_1, \dots, \sigma_{N-1}\rangle, \quad (2)$$

where the trace means contraction of the tensors. To obtain the ground state of the J_1 - J_2 Heisenberg model in Eq. (1), we apply the imaginary-time projection operator $\exp(-\tau H)$ repeatedly to an initial PEPS until convergence. As in Trotter-Suzuki decomposition [66], we first divide the lattice into four groups of plaquettes in a way that the projection operators of each plaquette within a group are independent or commute with each other. In each group, a projected entangled pair operator [PEPO; see Fig. 1(c)] for the projection operator within a single plaquette is constructed and is applied to the initial PEPS simultaneously. This procedure is carried out repeatedly for the four groups [see Fig. 1(d)]. Because the bond dimension increases after the application of the PEPO [67] [see Fig. 1(e)], we need to truncate it back to the original value D to make the calculation be under control [see Fig. 1(f)]. This

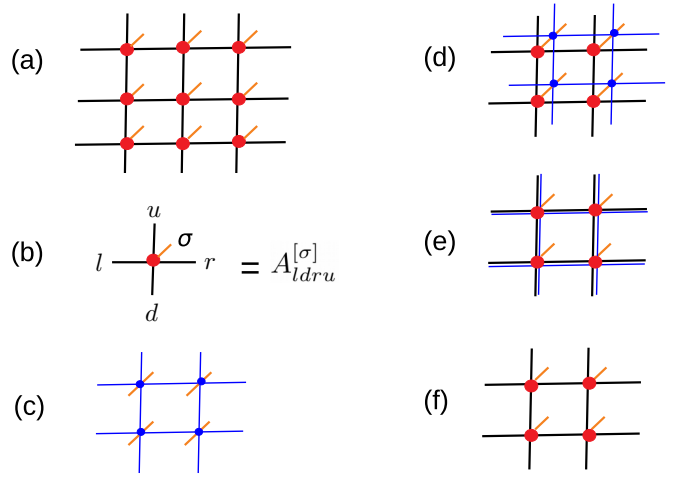


FIG. 1. PEPSs and the optimization process. (a) A PEPS on a square lattice, where there is a local tensor on each vertex. (b) The local tensor. The wave function is obtained by contracting all the auxiliary indexes. (c) PEPO for a plaquette. (d) The application of a PEPO to PEPS in a plaquette. (e) The bond dimension of PEPS is increased after the application of a PEPO; (f) The bond dimension is truncated back to the original value in (a).

is done in a variational fashion [68]. The whole procedure is a realization of the cluster update approach [69], which is a generalization of the simple update [25]. The most time-consuming part of this approach is the calculation of physical quantities after the PEPSs are optimized, which requires contraction of double-layer tensor networks with bond dimension D^2 . As we will discuss later, when combining PEPSs with GFMC, we need to calculate only single-layer tensor networks with bond dimension D , which reduces the complexity substantially. We notice the existence of a single-layer-like algorithm in the literature [70]. In the more sophisticated full update scheme of PEPS, the contraction of the double-layer tensor network is also needed in the optimization process [26,71].

IV. GREEN'S FUNCTION MONTE CARLO

In Green's function Monte Carlo [72–75], the ground state of a system is also obtained by the imaginary-time projection $|\psi_g\rangle \propto \lim_{\beta \rightarrow \infty} \exp(-\beta H) |\psi_0\rangle$. The projection length β is then divided into small slices with $\beta = M\tau$, with τ being a small number. In GFMC, we take the first-order expansion of the exponential function: $\exp(-\tau H) \propto C - H$, with C (or $1/\tau$) being a positive real number large enough to ensure all the diagonal elements of H are positive. Then the ground state can formally be written as $|\psi_g\rangle \propto \lim_{k \rightarrow \infty} K^k |\psi_0\rangle$, with $K = C - H$. A mixed estimate is employed in GFMC to calculate the ground state energy as $E = \frac{\langle \psi_g | H | \psi_g \rangle}{\langle \psi_g | \psi_g \rangle}$, which gives the exact ground state energy if $|\psi_g\rangle$ is the true ground state of H . Here we introduce a guiding wave function ψ_G whose effect will be discussed later. We use S to denote the spin configuration of the whole system, i.e., $S = (s_1^z, s_2^z, \dots, s_N^z)$, which is also the walker in the sampling process. We define the kernel as $\tilde{K}(S', S) = \psi_G^*(S') K(S', S) / \psi_G^*(S)$, with $K(S', S) = \langle S' | K | S \rangle$ and $\psi_G(S) = \langle S | \psi_G \rangle$. Then the ground state energy

from the mixed estimate is

$$E = \frac{\langle \psi_g | H | \psi_G \rangle}{\langle \psi_g | \psi_G \rangle} = \frac{\sum_{\{S\}} E_{\text{loc}}(S) \psi_G(S) \psi_g^*(S)}{\sum_{\{S\}} \psi_G(S) \psi_g^*(S)}, \quad (3)$$

where the local energy is defined as $E_{\text{loc}}(S) = \frac{\langle S | H | \psi_G \rangle}{\langle S | \psi_G \rangle}$. By introducing $f^*(S) = \psi_G^*(S) \psi_g(S)$, we have

$$E = \frac{\sum_{\{S\}} E_{\text{loc}}(S) f(S)}{\sum_{\{S\}} f(S)}. \quad (4)$$

So we can view $f(S)$ as probability density (if $f(S)$ is non-negative) and take advantage of Monte Carlo techniques, Metropolis, for example, to evaluate the summation in Eq. (4). It is easy to show $f^*(S) = \sum \tilde{K}(S, S_M) \tilde{K}(S_M, S_{M-1}) \cdots \tilde{K}(S_2, S_1) \psi_0(S_1) \psi_G^*(S_1)$ where the summation is over $\{S_1, S_2, \dots, S_M\}$.

The procedure of GFMC can be summarized as follows. At the first step, we sample S_1 according to $\psi_0(S_1) \psi_G^*(S_1)$ and set the weight of each walker to 1. This gives us an ensemble of walkers $\{S_1^i, \omega_1^i = 1\}$. We usually choose $\psi_0 = \psi_G$ and sample $\{S_1\}$ with probability $|\psi_G(S_1)|^2$. Then each walker $\{S_1^i, \omega_1^i\}$ is propagated to $\{S_2^i, \omega_2^i\}$ with probability $p(S_2^i) = \tilde{K}(S_2^i, S_1^i) / \beta_{2,1}^i$, where the normalization factor is $\beta_{2,1}^i = \sum_{S_2^i} \tilde{K}(S_2^i, S_1^i)$. After a new walker is chosen, we update the weight of it by multiplying the normalization factor as $\omega_2^i = \beta_{2,1}^i \omega_1^i$. This process is repeated, and we can start the measurement of energy after equilibrium is reached.

When the off-diagonal elements of H are all nonpositive, the ground state of H can be chosen to be non-negative according to the Perron-Frobenius theorem. Under this circumstance, $f(S)$ is non-negative if we choose an arbitrary non-negative guiding wave function because it is easy to prove the kernel $K(S', S)$ is non-negative. Then we can view $f(S)$ as the probability density without suffering from the negative sign problem.

For a Hamiltonian whose off-diagonal elements are not all negative, e.g., when the system is frustrated, we cannot ensure the non-negativeness of $f(S)$, and the negative sign problem emerges. Applying the fixed-node approximation [76] can solve this issue. With the fixed-node approximation, we actually study an effective Hamiltonian H_{eff} instead of the original Hamiltonian H . The off-diagonal of H_{eff} is defined as $\langle S' | H_{\text{eff}} | S \rangle = \langle S' | H | S \rangle$ if $\psi_G(S') H(S', S) / \psi_G^*(S) < 0$, and it is zero if $\psi_G(S') H(S', S) / \psi_G^*(S) \geq 0$, which means the off-diagonal elements causing the sign problem are discarded in H_{eff} . The diagonal part is defined as $\langle S | H_{\text{eff}} | S \rangle = \langle S | H | S \rangle + \langle S | V_{sf} | S \rangle$, with $\langle S | V_{sf} | S \rangle = \sum_{S'} \langle S | H | S' \rangle \frac{\psi_G(S')}{\psi_G(S)}$, where the summation is over all neighboring configurations S' of S for which $\psi_G(S') H(S', S) / \psi_G^*(S) > 0$. The effect of V_{sf} is a repulsion suppressing the wave function close to the node which is essential for the energy to be variational [76]. Different from the continuum system, both the sign and magnitude of the guiding wave function affect the accuracy in GFMC for lattice systems [76]. The off-diagonal elements of H_{eff} are now all nonpositive by definition, which allows us to obtain its ground state with GFMC without suffering from the negative sign problem. It can be proven GFMC is variational [76], and $E_{\text{eff}} \leq \langle \psi_G | H | \psi_G \rangle / \langle \psi_G | \psi_G \rangle$, which ensures GFMC gives a more accurate energy than the variational energy of ψ_G [76].

In practice, a fixed number of walkers is carried in the projection process [77], and a reconfiguration process is performed periodically [77] to reduce the fluctuation among walkers.

We can see that ψ_G serves as an important function in the GFMC sampling process when there is no sign problem. When the sign problem is present, ψ_G is also used to control the sign problem. So the quality of ψ_G controls both the accuracy and efficiency of GFMC. PEPSs are known to be accurate wave function for 2D systems, which makes them good candidates for ψ_G . In GFMC, we need to calculate only the overlap between ψ_G and walker, which is a tensor network also with bond dimension D , while in the calculation of the physical quantities of PEPSs, contraction of the double-layer tensor network with bond dimension D^2 is needed. Although it is known that the rigorous contraction of the tensor network in two dimensions is fundamentally difficult [78], many effective approximate algorithms exist [68,79–86] in the literature.

This work is not the first time TNS and GFMC have been combined. Many attempts have been made in the past to either optimize tensor network states [87–92] with Monte Carlo techniques or to take MPSs as a guiding [93] or trial wave function [94] to control the negative sign problem. The advance in our work is that we take true 2D TNSs, PEPSs, as the guiding wave function in GFMC, which can reduce the cost of PEPS substantially and at the same time improve the accuracy over PEPS.

V. RESULTS

It is known that the Heisenberg model without the J_2 term is sign problem free [72–75]. By a rotation of the spin along the z axis on one sublattice, the sign of the coupling for x and y components is flipped, and the off-diagonal elements of H in Eq. (1) are all negative. This is the so-called Marshall sign in the ground state of the Heisenberg model [95] on bipartite lattices. In the following, we show benchmark results for both $J_2 = 0$ and $J_2 \neq 0$ for 4×4 and 6×6 lattice sizes. The “exact” ground state energies are from DMRG with a truncation error below 10^{-8} and with an extrapolation to zero truncation error.

In Fig. 2 we show results for $J_2 = 0$ on a 4×4 lattice with open boundary conditions. We first obtain a $D = 4$ PEPS with cluster update, which gives $E_{D=4} = -9.034333$. We then carry out a GFMC calculation with this PEPS as the guiding wave function. As we can see from Fig. 2, the final converged energy $[-9.189(1)]$ matches the exact energy (-9.189207) within the error bars, which is reasonable because there is no negative sign problem here. When there is no sign problem, the guiding PEPS wave function plays the role of an important function whose quality affects only the sampling efficiency in GFMC.

We then move to the more challenging $J_2 \neq 0$ case, where the negative sign problem emerges and we need to employ the fixed-node approximation. In Fig. 3, we show the GFMC results for a system on a 6×6 lattice with OBCs and $J_2 = 0.5$, which represents the most difficult region of the J_1 - J_2 Heisenberg model. A PEPS with $D = 4$ from the cluster update is taken as the guiding wave function in GFMC. The variational energy for the $D = 4$ PEPS is $-16.763(4)$, while the energy

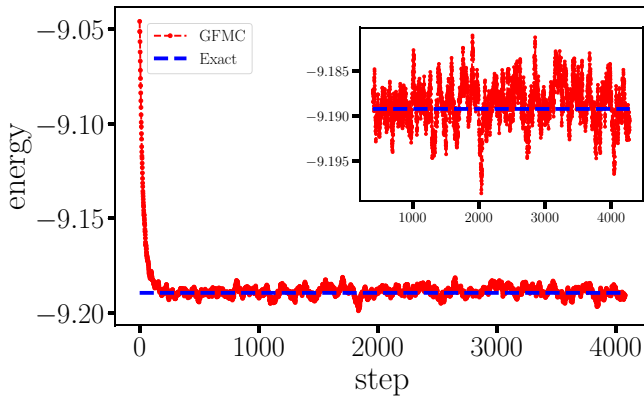


FIG. 2. Energy versus step in the GFMC calculation for a 4×4 , $J_2 = 0$ system with OBCs. A PEPS with bond dimension $D = 4$ is used as the guiding function. The energy at step 0 is the variation energy of the $D = 4$ PEPS, which is -9.034333 . There is no sign problem in this case, so GFMC should give numerically exact energy. The exact energy is -9.189207 , as indicated by the blue dashed line, while the GFMC energy is $-9.189(1)$. The inset shows a zoom of the energy after equilibrium.

from GFMC is $-16.965(1)$. This means the error to the exact energy (-17.24733) is reduced nearly by half with GFMC in this case. In Fig. 4 we show a comparison of the converged GFMC energy and the energy of the corresponding PEPS guiding wave function for a range of bond dimensions. We can see for all D values that the GFMC energies are lower than PEPS energy and the errors are reduced by about 40%. We want to emphasize that $J_2 = 0.5$ is the most difficult region for the J_1 - J_2 Heisenberg model. We anticipate that the improvement in other regions will be even larger (the $J_2 = 0$ result above is an example).

Usually in the GFMC calculation, a variational Monte Carlo (VMC) calculation is performed first to obtain the guiding wave function [75]. TNSs can also be viewed as variational wave functions. Nevertheless, the form of the wave function needs to be specified in VMC, while TNSs are more

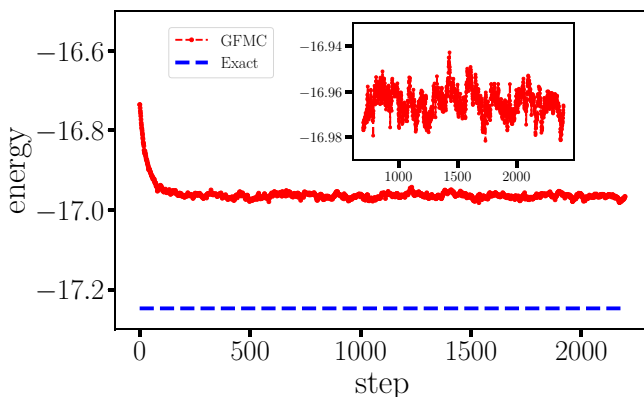


FIG. 3. Same as Fig. 2, but for energy of a 6×6 system with OBCs and $J_2 = 0.5$. The guiding wave function is a $D = 4$ PEPS with variational energy $-16.763(4)$ (the energy at step 0). The GFMC energy is $-16.965(1)$, and exact energy (the blue dashed line) for this system is -17.24733 .

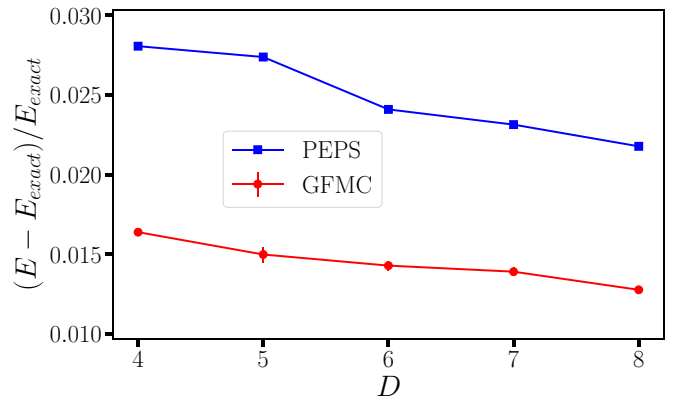


FIG. 4. Comparison of the GFMC energy and the energy of the corresponding PEPS guiding wave functions for a range of bond dimensions. The relative error of the energy is shown. The system size is 6×6 , and $J_2 = 0.5$.

general and are systematically improvable with the increase of bond dimension D [29]. Moreover, PEPSs satisfy the area law [24] by design.

VI. SUMMARY AND PERSPECTIVES

In conclusion, we proposed an approach to study the ground state properties of quantum many-body systems in which TNSs and GFMC are combined to take advantage of both of them. Benchmark results for the J_1 - J_2 Heisenberg model on a square lattice were provided to demonstrate the effectiveness of this method. One benefit to combine PEPSs and GFMC is that only contraction of the single-layer tensor network is needed, which reduces the computational complexity substantially (from D^{12} to D^6) and enables the reach of the large bond dimension in PEPSs if the optimization process does not involve contraction of the double-layer tensor network. Nevertheless, after obtaining the optimized PEPSs with a full update, we can further improve the energy by taking it as the guiding wave function, although the bottleneck is the optimization of the PEPS itself in the full update. The energy obtained in GFMC is guaranteed to be variational and lower than the PEPS guiding wave function. Our method can be improved in many aspects. With the stochastic reconfiguration technique [96], the bias from the guiding wave function can be reduced. We can generalize the single PEPS guiding function to a linear combination of PEPSs [97], which can give lower variational energy. Generalization to fermionic systems is straightforward [46,47]. We calculated only the ground state energy in this work, but excitation gaps can be calculated easily by enforcing symmetry, conservation of S_z^{tot} , for example, in PEPSs. Quantities other than energy can be calculated with the forward propagation technique [75] without increasing computational complexity. Tensor network states other than PEPSs [98–100] can also be adopted as the guiding wave function. We believe that this approach will provide us an accurate and efficient tool in the study of strongly correlated many-body systems in the future.

ACKNOWLEDGMENTS

This work is supported by a start-up fund from the School of Physics and Astronomy at Shanghai Jiao Tong University.

I thank S. Zhang for previous discussions about the combination of TNSs and QMC. I also acknowledge the support of computational resources by S. Zhang at the Flatiron Institute.

- [1] J. G. Bednorz and K. A. Müller, *Z. Phys. B* **64**, 189 (1986).
- [2] D. C. Tsui, H. L. Stormer, and A. C. Gossard, *Phys. Rev. Lett.* **48**, 1559 (1982).
- [3] R. B. Laughlin, *Phys. Rev. Lett.* **50**, 1395 (1983).
- [4] Y. Zhou, K. Kanoda, and T.-K. Ng, *Rev. Mod. Phys.* **89**, 025003 (2017).
- [5] E. H. Lieb and F. Y. Wu, *Phys. Rev. Lett.* **20**, 1445 (1968).
- [6] S. R. White, *Phys. Rev. Lett.* **69**, 2863 (1992).
- [7] S. R. White, *Phys. Rev. B* **48**, 10345 (1993).
- [8] U. Schollwöck, *Rev. Mod. Phys.* **77**, 259 (2005).
- [9] U. Schollwöck, *Ann. Phys. (N.Y.)* **326**, 96 (2011).
- [10] S. Östlund and S. Rommer, *Phys. Rev. Lett.* **75**, 3537 (1995).
- [11] I. Affleck, T. Kennedy, E. H. Lieb, and H. Tasaki, *Phys. Rev. Lett.* **59**, 799 (1987).
- [12] R. J. Baxter, *J. Math. Phys.* **9**, 650 (1968).
- [13] J. Eisert, M. Cramer, and M. B. Plenio, *Rev. Mod. Phys.* **82**, 277 (2010).
- [14] F. Verstraete, V. Murg, and J. Cirac, *Adv. Phys.* **57**, 143 (2008).
- [15] R. Orús, *Ann. Phys. (N.Y.)* **349**, 117 (2014).
- [16] X. Chen, Z.-C. Gu, and X.-G. Wen, *Phys. Rev. B* **83**, 035107 (2011).
- [17] N. Schuch, D. Pérez-García, and I. Cirac, *Phys. Rev. B* **84**, 165139 (2011).
- [18] E. Stoudenmire and S. R. White, *Annu. Rev. Condens. Matter Phys.* **3**, 111 (2012).
- [19] S. Yan, D. A. Huse, and S. R. White, *Science* **332**, 1173 (2011).
- [20] J. P. F. Le Blanc, A. E. Antipov, F. Becca, I. W. Bulik, Garnet Kin-Lic Chan, C. M. Chung, Y. Deng, M. Ferrero, T. M. Henderson, C. A. Jimenez-Hoyos, E. Kozik, X. W. Liu, A. J. Millis, N. V. Prokofev, M. Qin, G. E. Scuseria, H. Shi, B. V. Svistunov, L. F. Tocchio, I. S. Tupitsyn, S. R. White, S. Zhang, B. X. Zheng, Z. Zhu, and E. Gull (Simons Collaboration on the Many-Electron Problem), *Phys. Rev. X* **5**, 041041 (2015).
- [21] B.-X. Zheng, C.-M. Chung, P. Corboz, G. Ehlers, M.-P. Qin, R. M. Noack, H. Shi, S. R. White, S. Zhang, and G. K.-L. Chan, *Science* **358**, 1155 (2017).
- [22] M. Qin, C.-M. Chung, H. Shi, E. Vitali, C. Hubig, U. Schollwöck, S. R. White, and S. Zhang (Simons Collaboration on the Many-Electron Problem), *Phys. Rev. X* **10**, 031016 (2020).
- [23] S. Liang and H. Pang, *Phys. Rev. B* **49**, 9214 (1994).
- [24] F. Verstraete and J. I. Cirac, [arXiv:cond-mat/0407066](https://arxiv.org/abs/cond-mat/0407066).
- [25] H. C. Jiang, Z. Y. Weng, and T. Xiang, *Phys. Rev. Lett.* **101**, 090603 (2008).
- [26] J. Jordan, R. Orús, G. Vidal, F. Verstraete, and J. I. Cirac, *Phys. Rev. Lett.* **101**, 250602 (2008).
- [27] P. Corboz, A. M. Läuchli, K. Penc, M. Troyer, and F. Mila, *Phys. Rev. Lett.* **107**, 215301 (2011).
- [28] P. Corboz, T. M. Rice, and M. Troyer, *Phys. Rev. Lett.* **113**, 046402 (2014).
- [29] H. J. Liao, Z. Y. Xie, J. Chen, Z. Y. Liu, H. D. Xie, R. Z. Huang, B. Normand, and T. Xiang, *Phys. Rev. Lett.* **118**, 137202 (2017).
- [30] D. Gioev and I. Klich, *Phys. Rev. Lett.* **96**, 100503 (2006).
- [31] R. Orús and G. Vidal, *Phys. Rev. B* **80**, 094403 (2009).
- [32] H. N. Phien, J. A. Bengua, H. D. Tuan, P. Corboz, and R. Orús, *Phys. Rev. B* **92**, 035142 (2015).
- [33] Y. Ran, M. Hermele, P. A. Lee, and X.-G. Wen, *Phys. Rev. Lett.* **98**, 117205 (2007).
- [34] S. Depenbrock, I. P. McCulloch, and U. Schollwöck, *Phys. Rev. Lett.* **109**, 067201 (2012).
- [35] Y. Iqbal, F. Becca, S. Sorella, and D. Poilblanc, *Phys. Rev. B* **87**, 060405(R) (2013).
- [36] J.-W. Mei, J.-Y. Chen, H. He, and X.-G. Wen, *Phys. Rev. B* **95**, 235107 (2017).
- [37] R. Blankenbecler, D. J. Scalapino, and R. L. Sugar, *Phys. Rev. D* **24**, 2278 (1981).
- [38] F. F. Assaad and H. G. Evertz, in *Computational Many Particle Physics*, Lecture Notes in Physics Vol. 739, edited by H. Fehske, R. Schneider, and A. Weiße (Springer Verlag, Berlin, 2008), p. 277.
- [39] S. Zhang, *Quantum Monte Carlo Methods for Strongly Correlated Electron Systems* (Springer, New York, 2004), pp. 39–74.
- [40] E. Y. Loh, J. E. Gubernatis, R. T. Scalettar, S. R. White, D. J. Scalapino, and R. L. Sugar, *Phys. Rev. B* **41**, 9301 (1990).
- [41] M. Troyer and U.-J. Wiese, *Phys. Rev. Lett.* **94**, 170201 (2005).
- [42] M. H. Kalos, *Phys. Rev.* **128**, 1791 (1962).
- [43] D. M. Ceperley and B. J. Alder, *Phys. Rev. Lett.* **45**, 566 (1980).
- [44] W. M. C. Foulkes, L. Mitás, R. J. Needs, and G. Rajagopal, *Rev. Mod. Phys.* **73**, 33 (2001).
- [45] S. Zhang, J. Carlson, and J. E. Gubernatis, *Phys. Rev. B* **55**, 7464 (1997).
- [46] G. An and J. M. J. van Leeuwen, *Phys. Rev. B* **44**, 9410 (1991).
- [47] H. J. M. van Bemmelen, D. F. B. ten Haaf, W. van Saarloos, J. M. J. van Leeuwen, and G. An, *Phys. Rev. Lett.* **72**, 2442 (1994).
- [48] L. Capriotti, A. E. Trumper, and S. Sorella, *Phys. Rev. Lett.* **82**, 3899 (1999).
- [49] C.-C. Chang and S. Zhang, *Phys. Rev. B* **78**, 165101 (2008).
- [50] M. Qin, H. Shi, and S. Zhang, *Phys. Rev. B* **94**, 235119 (2016).
- [51] P. Chandra and B. Douçot, *Phys. Rev. B* **38**, 9335 (1988).
- [52] E. Dagotto and A. Moreo, *Phys. Rev. Lett.* **63**, 2148 (1989).
- [53] L. Capriotti and S. Sorella, *Phys. Rev. Lett.* **84**, 3173 (2000).
- [54] A. W. Sandvik, *Phys. Rev. B* **56**, 11678 (1997).
- [55] F.-J. Jiang and U.-J. Wiese, *Phys. Rev. B* **83**, 155120 (2011).
- [56] A. W. Sandvik and H. G. Evertz, *Phys. Rev. B* **82**, 024407 (2010).
- [57] M. Mambrini, A. Läuchli, D. Poilblanc, and F. Mila, *Phys. Rev. B* **74**, 144422 (2006).

- [58] V. Murg, F. Verstraete, and J. I. Cirac, *Phys. Rev. B* **79**, 195119 (2009).
- [59] J.-F. Yu and Y.-J. Kao, *Phys. Rev. B* **85**, 094407 (2012).
- [60] H.-C. Jiang, H. Yao, and L. Balents, *Phys. Rev. B* **86**, 024424 (2012).
- [61] F. Mezzacapo, *Phys. Rev. B* **86**, 045115 (2012).
- [62] W.-J. Hu, F. Becca, A. Parola, and S. Sorella, *Phys. Rev. B* **88**, 060402(R) (2013).
- [63] S.-S. Gong, W. Zhu, D. N. Sheng, O. I. Motrunich, and M. P. A. Fisher, *Phys. Rev. Lett.* **113**, 027201 (2014).
- [64] S. Morita, R. Kaneko, and M. Imada, *J. Phys. Soc. Jpn.* **84**, 024720 (2015).
- [65] L. Wang and A. W. Sandvik, *Phys. Rev. Lett.* **121**, 107202 (2018).
- [66] M. Suzuki, *Prog. Theor. Phys.* **56**, 1454 (1976).
- [67] B. Pirvu, V. Murg, J. I. Cirac, and F. Verstraete, *New J. Phys.* **12**, 025012 (2010).
- [68] G. Evenbly, *Phys. Rev. B* **98**, 085155 (2018).
- [69] L. Wang and F. Verstraete, [arXiv:1110.4362](https://arxiv.org/abs/1110.4362).
- [70] Z. Y. Xie, H. J. Liao, R. Z. Huang, H. D. Xie, J. Chen, Z. Y. Liu, and T. Xiang, *Phys. Rev. B* **96**, 045128 (2017).
- [71] P. Corboz, R. Orús, B. Bauer, and G. Vidal, *Phys. Rev. B* **81**, 165104 (2010).
- [72] J. Carlson, *Phys. Rev. B* **40**, 846 (1989).
- [73] N. Trivedi and D. M. Ceperley, *Phys. Rev. B* **40**, 2737 (1989).
- [74] N. Trivedi and D. M. Ceperley, *Phys. Rev. B* **41**, 4552 (1990).
- [75] K. J. Runge, *Phys. Rev. B* **45**, 7229 (1992).
- [76] D. F. B. ten Haaf, H. J. M. van Bemmelen, J. M. J. van Leeuwen, W. van Saarloos, and D. M. Ceperley, *Phys. Rev. B* **51**, 13039 (1995).
- [77] M. Calandra Buonaura and S. Sorella, *Phys. Rev. B* **57**, 11446 (1998).
- [78] N. Schuch, M. M. Wolf, F. Verstraete, and J. I. Cirac, *Phys. Rev. Lett.* **98**, 140506 (2007).
- [79] T. Nishino and K. Okunishi, *J. Phys. Soc. Jpn.* **65**, 891 (1996).
- [80] M. Levin and C. P. Nave, *Phys. Rev. Lett.* **99**, 120601 (2007).
- [81] Z.-C. Gu and X.-G. Wen, *Phys. Rev. B* **80**, 155131 (2009).
- [82] H. H. Zhao, Z. Y. Xie, Q. N. Chen, Z. C. Wei, J. W. Cai, and T. Xiang, *Phys. Rev. B* **81**, 174411 (2010).
- [83] M. Lubasch, J. I. Cirac, and M.-C. Bañuls, *Phys. Rev. B* **90**, 064425 (2014).
- [84] Z. Y. Xie, J. Chen, M. P. Qin, J. W. Zhu, L. P. Yang, and T. Xiang, *Phys. Rev. B* **86**, 045139 (2012).
- [85] G. Evenbly and G. Vidal, *Phys. Rev. Lett.* **115**, 180405 (2015).
- [86] S. Yang, Z.-C. Gu, and X.-G. Wen, *Phys. Rev. Lett.* **118**, 110504 (2017).
- [87] A. W. Sandvik and G. Vidal, *Phys. Rev. Lett.* **99**, 220602 (2007).
- [88] N. Schuch, M. M. Wolf, F. Verstraete, and J. I. Cirac, *Phys. Rev. Lett.* **100**, 040501 (2008).
- [89] L. Wang, I. Pižorn, and F. Verstraete, *Phys. Rev. B* **83**, 134421 (2011).
- [90] O. Sikora, H.-W. Chang, C.-P. Chou, F. Pollmann, and Y.-J. Kao, *Phys. Rev. B* **91**, 165113 (2015).
- [91] W.-Y. Liu, S.-J. Dong, Y.-J. Han, G.-C. Guo, and L. He, *Phys. Rev. B* **95**, 195154 (2017).
- [92] H.-H. Zhao, K. Ido, S. Morita, and M. Imada, *Phys. Rev. B* **96**, 085103 (2017).
- [93] M. S. L. du Croo de Jongh, J. M. J. van Leeuwen, and W. van Saarloos, *Phys. Rev. B* **62**, 14844 (2000).
- [94] S. Wouters, B. Verstichel, D. Van Neck, and G. K.-L. Chan, *Phys. Rev. B* **90**, 045104 (2014).
- [95] W. Marshall and R. E. Peierls, *Proc. R. Soc. London, Ser. A* **232**, 48 (1955).
- [96] S. Sorella and L. Capriotti, *Phys. Rev. B* **61**, 2599 (2000).
- [97] R.-Z. Huang, H.-J. Liao, Z.-Y. Liu, H.-D. Xie, Z.-Y. Xie, H.-H. Zhao, J. Chen, and T. Xiang, *Chin. Phys. B* **27**, 070501 (2018).
- [98] Y.-Y. Shi, L.-M. Duan, and G. Vidal, *Phys. Rev. A* **74**, 022320 (2006).
- [99] G. Vidal, *Phys. Rev. Lett.* **101**, 110501 (2008).
- [100] Z. Y. Xie, J. Chen, J. F. Yu, X. Kong, B. Normand, and T. Xiang, *Phys. Rev. X* **4**, 011025 (2014).